

Engineering Notes

Model for Linearized Satellite Relative Motion About a J_2 -Perturbed Mean Circular Orbit

Srinivas R. Vadali*

Texas A&M University, College Station, Texas 77843-3141

DOI: 10.2514/1.42955

Introduction

SEVERAL previous studies [1–4] have reported on the development of linear differential equations for modeling J_2 -perturbed relative motion of satellites with respect to a circular orbit. Such equations allow for a direct simulation of relative motion and are useful for parametric studies. Moreover, linear differential equations with periodic coefficients are amenable to mathematical analysis by Floquet theory and the application of tailored control methods. Relative motion equations typically involve the orbital radius of the reference satellite (often designated as the chief) and the angular velocities of the chief-fixed rotating reference frame; these are functions of a set of orbital elements. The relative motion model developed by Vadali et al. [1] accounts for the secular perturbations of the elements, but not their short-period variations. This model also neglects the coupling terms between the out-of-plane and in-plane equations, leading to a loss of precision. Ross [2] appends the differential J_2 accelerations as forcing functions to the Clohessy–Wiltshire equations, but the perturbations to the two-body mean motion and the angular rates of the reference frame are not accounted for. Schweigart and Sedwick [3] include the orbit-averaged absolute and differential perturbations; however, they do not treat the short-period effects in a comprehensive manner. Izzo et al. [4] an ad hoc approach for modeling the short-period effects. Their model is based on approximations to the angular momentum and radius of the chief's orbit, derived by assuming a constant reference orbit inclination and the use of the two-body mean motion instead of the perturbed mean motion; furthermore, their model requires the specifications of the initial osculating elements of the chief. A consistent incorporation of the mean elements and their short-period variations into the relative motion equations is the subject of this paper.

Gim and Alfriend [5] provide a state transition matrix (STM) for propagating the relative motion states (relative position and velocity vectors) for elliptic reference orbits in a curvilinear coordinate system. Underlying their development are the STMs for propagating the differential nonsingular as well as the differential equinoctial orbital elements. However, the expressions for building the STMs are complicated due to the presence of the short- and long-period effects of J_2 . There are no long-period effects of the J_2 perturbation on the elements of a mean circular orbit. The long-period terms for elliptic orbits can be ignored for simplifying the STM, especially for prediction times less than the perigee rotation period. Hamel and

Received 27 December 2008; accepted for publication 17 June 2009. Copyright © 2009 by Srinivas R. Vadali. Published by the American Institute of Aeronautics and Astronautics, Inc., with permission. Copies of this paper may be made for personal or internal use, on condition that the copier pay the \$10.00 per-copy fee to the Copyright Clearance Center, Inc., 222 Rosewood Drive, Danvers, MA 01923; include the code 0731-5090/09 and \$10.00 in correspondence with the CCC.

*Stewart & Stevenson-I Professor, Department of Aerospace Engineering, MS 3141; svadali@aero.tamu.edu. Associate Fellow AIAA.

Lafontaine [6] consider such an alternative, but the fundamental matrix derived suffers from a singularity for zero mean eccentricity of the reference orbit. Born et al. [7] derive short-period corrections to the mean nonsingular orbital elements for near-circular orbits using the principle of averaging. Sengupta et al. [8] also derive such corrections for elliptic orbits by the application of the Brouwer theory [9]. There exist minor differences between the expressions for the short-period corrections, for the special case of the mean circular orbit, derived in [7], and the corresponding results of [8].

In this paper, a set of linearized relative motion equations are derived with respect to a mean circular reference orbit by using expressions for the secular drift rates and the short-period variations of the chief's orbital elements as given in [8]. The structure of the model developed in this paper is the same as that of [4], the differences are in the short-period approximations used. The accuracy of the developed model is evaluated by comparison with the data obtained from simulating the nonlinear equations of motion of the individual satellites and computing the relative motion therefrom. The secular in-track linearization error of the model is shown to be consistent with the estimate given in Vaddi et al. [10] for unperturbed relative motion, rendering the J_2 -induced errors to be predominantly periodic in nature.

Development of the Model

A mean circular reference orbit and a rotating reference frame are chosen to express the relative motion equations in the phase space comprising the relative position and velocity vectors. The relative position vector of a deputy satellite defined in the chief-fixed rotating coordinate system is denoted by

$$\delta\mathbf{r} = [x \ y \ z]^T \quad (1)$$

where x , y , and z are, respectively, the radial, in-track, and cross-track position coordinates. The angular velocity vector of the rotating frame is

$$\boldsymbol{\omega} = [\omega_x \ \omega_y \ \omega_z]^T \quad (2)$$

with

$$\omega_x = \dot{\Omega}_0 \sin i_0 \sin \theta_0 + \dot{i}_0 \cos \theta_0 \quad (3a)$$

$$\omega_y = \dot{\Omega}_0 \sin i_0 \cos \theta_0 - \dot{i}_0 \sin \theta_0 \quad (3b)$$

$$\omega_z = \dot{\Omega}_0 \cos i_0 + \dot{\theta}_0 \quad (3c)$$

where Ω_0 is the longitude of the ascending node, θ_0 is the argument of latitude, and i_0 is the inclination of the reference orbit. Equations (3a–3c) are written in terms of the osculating elements.

The nonlinear equations of perturbed relative motion [4] are

$$\ddot{\delta\mathbf{r}} = -2\boldsymbol{\omega} \times \dot{\delta\mathbf{r}} - \boldsymbol{\omega} \times (\boldsymbol{\omega} \times \delta\mathbf{r}) - \dot{\boldsymbol{\omega}} \times \delta\mathbf{r} + \nabla F_{g2B} + \nabla F_{gJ_2} \quad (4)$$

where ∇F_{g2B} is the gravity gradient acceleration due to the two-body gravity field and ∇F_{gJ_2} is that due to the J_2 potential. The two-body gravity gradient acceleration, expressed in the rotating reference frame, is [10]

$$\nabla F_{g2B} = -\mu \left[\begin{array}{c} \frac{(r_0+x)}{\{(r_0+x)^2+y^2+z^2\}^{\frac{3}{2}}} - \frac{1}{r_0^2} \\ \frac{y}{\{(r_0+x)^2+y^2+z^2\}^{\frac{3}{2}}} \\ \frac{z}{\{(r_0+x)^2+y^2+z^2\}^{\frac{3}{2}}} \end{array} \right] \quad (5)$$

where μ is the gravitational parameter and r_0 is the radius of the chief's orbit. Equation (5) can be linearized about r_0 to obtain

$$\nabla F_{g2B} \approx -\frac{\mu}{r_0^3} \begin{bmatrix} -2x \\ y \\ z \end{bmatrix} \quad (6)$$

The linearized J_2 differential acceleration vector is [4]

$$\nabla F_{gJ_2} = G \begin{bmatrix} 1 - 3\sin^2 i_0 \sin^2 \theta_0 & \sin^2 i_0 \sin 2\theta_0 & \sin 2i_0 \sin \theta_0 \\ \sin^2 i_0 \sin 2\theta_0 & -\frac{1}{4} + \sin^2 i_0 (\frac{7}{4} \sin^2 \theta_0 - \frac{1}{2}) & -\frac{1}{4} \sin 2i_0 \cos \theta_0 \\ \sin 2i_0 \sin \theta_0 & -\frac{1}{4} \sin 2i_0 \cos \theta_0 & -\frac{3}{4} + \sin^2 i_0 (\frac{5}{4} \sin^2 \theta_0 + \frac{1}{2}) \end{bmatrix} \delta \mathbf{r} \quad (7)$$

where \bar{a}_0 is the mean semimajor axis, $G = 6n_0^2 J_2 (\bar{a}_0 / r_0)^3$, and n_0 is the two-body mean motion, based on \bar{a}_0 .

Short-Period Effects

The relationships between the osculating and mean elements for mean circular orbits can be obtained from the detailed expressions given in [5]. These expressions are also available in [8] in a convenient form. The relevant variables for the case of circular orbits, derived from those given in [8], are

$$r_0 = \bar{a}_0 [1 + J_2 (\frac{3}{4} (1 - 3\cos^2 \bar{i}_0) + \frac{1}{4} \sin^2 \bar{i}_0 \cos 2\bar{\theta}_0)] \quad (8a)$$

$$\theta_0 = \bar{\theta}_0(0) + \dot{\bar{\theta}}_0 t + \frac{1}{8} J (1 - 7\cos^2 \bar{i}_0) \sin 2\bar{\theta}_0 \quad (8b)$$

$$i_0 = \bar{i}_0 + \frac{3}{8} J \sin 2\bar{i}_0 \cos 2\bar{\theta}_0 \quad (8c)$$

$$\Omega_0 = \bar{\Omega}_0(0) + \dot{\bar{\Omega}}_0 t + \frac{3}{4} J \cos \bar{i}_0 \sin 2\bar{\theta}_0 \quad (8d)$$

where $\bar{\theta}_0 = \bar{\theta}_0(0) + \dot{\bar{\theta}}_0 t$, $J = J_2 (R_e / \bar{a}_0)^2$, and

$$\dot{\bar{\theta}}_0 = n_0 \left[1 - \frac{3}{2} J (1 - 4\cos^2 \bar{i}_0) \right] \quad (9a)$$

$$\dot{\bar{\Omega}}_0 = -\frac{3}{2} J n_0 \cos \bar{i}_0 \quad (9b)$$

Substitution of Eqs. (8b–8d), (9a), and (9b) into Eqs. (3a–3c) and the approximation $\theta_0 \approx \bar{\theta}_0$ in the evaluation of the trigonometric functions therein results in the following expressions for the angular velocities:

$$\omega_x = 2\dot{\bar{\Omega}}_0 \sin \bar{i}_0 \sin \bar{\theta}_0 \quad (10a)$$

$$\omega_y = 0 \quad (10b)$$

$$\omega_z = \dot{\bar{\Omega}}_0 \cos \bar{i}_0 + \dot{\bar{\theta}}_0 + \frac{1}{4} J n_0 \cos 2\bar{\theta}_0 \sin^2 \bar{i}_0 \quad (10c)$$

The mean element approximation is performed by setting $\dot{\bar{\Omega}}_0 = \dot{\bar{\Omega}}_0$, $\dot{\bar{\theta}}_0 = \dot{\bar{\theta}}_0$, and $\dot{i}_0 = 0$ in Eqs. (3a–3c). Note that the two expressions for ω_x given by Eqs. (10a) and (3a), with the mean element approximation, differ by a factor of 2. Equation (10b) shows that the approximations developed in this section satisfy the osculating orbit condition of Eq. (3b). The short-period correction to the mean ω_z is obvious from Eq. (10c).

Linear Model

The relative motion equations are assembled in a matrix form by substituting the relevant expressions derived previously into Eq. (4), including the linear approximation to ∇F_{g2B} given by Eq. (6). Although the structure of the model presented is the same as that given in [4], the expressions for the orbital radius and angular velocities used are as derived in this paper. The linear model is

$$\begin{bmatrix} \dot{\delta \mathbf{r}} \\ \ddot{\delta \mathbf{r}} \end{bmatrix} = \begin{bmatrix} 0 & 0 & 0 & 1 & 0 & 0 \\ 0 & 0 & 0 & 0 & 1 & 0 \\ 0 & 0 & 0 & 0 & 0 & 1 \\ a_{41} & a_{42} & a_{43} & 0 & 2\omega_z & 0 \\ a_{51} & a_{52} & a_{53} & -2\omega_z & 0 & 2\omega_x \\ a_{61} & a_{62} & a_{63} & 0 & -2\omega_x & 0 \end{bmatrix} \begin{bmatrix} \delta \mathbf{r} \\ \dot{\delta \mathbf{r}} \end{bmatrix} \quad (11)$$

where

$$a_{41} = \omega_z^2 + 2\frac{\mu}{r_0^3} + G(1 - 3\sin^2 \bar{i}_0 \sin^2 \bar{\theta}_0) \quad (12a)$$

$$a_{42} = \dot{\omega}_z + G(\sin^2 \bar{i}_0 \sin 2\bar{\theta}_0) \quad (12b)$$

$$a_{43} = -\omega_x \omega_z + G(\sin 2\bar{i}_0 \sin \bar{\theta}_0) \quad (12c)$$

$$a_{51} = -\dot{\omega}_z + G(\sin^2 \bar{i}_0 \sin 2\bar{\theta}_0) \quad (12d)$$

$$a_{52} = \omega_x^2 + \omega_z^2 - \frac{\mu}{r_0^3} + G[-\frac{1}{4} + \sin^2 \bar{i}_0 (\frac{7}{4} \sin^2 \bar{\theta}_0 - \frac{1}{2})] \quad (12e)$$

$$a_{53} = \dot{\omega}_x - G(\frac{1}{4} \sin 2\bar{i}_0 \cos \bar{\theta}_0) \quad (12f)$$

$$a_{61} = -\omega_x \omega_z + G(\sin 2\bar{i}_0 \sin \bar{\theta}_0) \quad (12g)$$

$$a_{62} = -\dot{\omega}_x - G(\frac{1}{4} \sin 2\bar{i}_0 \cos \bar{\theta}_0) \approx 0 \quad (12h)$$

$$a_{63} = \omega_x^2 - \frac{\mu}{r_0^3} + G[-\frac{3}{4} + \sin^2 \bar{i}_0 (\frac{5}{4} \sin^2 \bar{\theta}_0 + \frac{1}{2})] \quad (12i)$$

Equations (12) can be simplified further by making several approximations. For example, it can be shown that $a_{62} \approx 0$ to $\mathcal{O}(J_2)$. The in-track y motion is sensitive to the term a_{53} , especially for initial conditions corresponding to a nonzero nodal difference between the two satellites, $\delta\Omega(0) \neq 0$. This shows the existence of a coupling between cross-track and in-track variables for certain initial conditions. Another observation is that the terms involving μ/r_0^3 in Eq. (12) can be reduced by using a binomial expansion of $\mathcal{O}(J_2)$. However, this simplification increases the propagation errors over the long run, leading to the conclusion that, where possible, terms of $\mathcal{O}(J_2^2)$ and higher should be retained.

Numerical Simulations

The reference orbit selected for the numerical simulations has the following initial mean nonsingular orbital elements:

$$\begin{aligned} \bar{a}_0 &= 7100 \text{ km}, & \bar{\theta}_0 &= 0, & \bar{i}_0 &= 70 \text{ deg} \\ \bar{q}_{10} &= 0, & \bar{q}_{20} &= 0, & \bar{\Omega}_0 &= 45 \text{ deg} \end{aligned}$$

The deputy is set up in a projected circular orbit (PCO) in the examples to follow. The initial conditions for setting up such a relative orbit, parameterized by ρ , the radius of the PCO, and α_0 , the initial phase angle, are obtained from [11,12]. For model verification, nonlinear simulations are performed by integrating the equations of motion of the two satellites in the earth-centered-inertial (ECI) frame and the nonlinear relative motion results are obtained from the transformations given in [13]. Several numerical examples are presented next.

Case 1. The following initial conditions on the state variables are obtained for a PCO with $\rho = 0.5$ km and $\alpha_0 = 0$:

$$\begin{aligned} \delta\mathbf{r}(0) &= \\ &[-0.000288947081 \ 0.500033326318 \ 0.000175666681]^T \text{ km} \\ \dot{\delta}\mathbf{r}(0) &= \\ &[0.000263388377 \ 0.000000272412 \ 0.000527371445]^T \text{ km/s} \end{aligned}$$

The corresponding initial conditions of the chief and deputy in the ECI frame are

$$\begin{aligned} \mathbf{r}_0 &= [5023.558528005 \ 5023.558528005 \ 0]^T \text{ km} \\ \mathbf{v}_0 &= \\ &[-1.810956397226 \ 1.810956397226 \ 7.041120373157]^T \text{ km/s} \\ \mathbf{r}_1 &= [5023.437579954 \ 5023.679067423 \ 0.469973680]^T \text{ km} \\ \mathbf{v}_1 &= \\ &[-1.810792589537 \ 1.810419297938 \ 7.041300610075]^T \text{ km/s} \end{aligned}$$

The errors in the three components of $\delta\mathbf{r}$ between the linear and the nonlinear simulation results are shown in Fig. 1. The radial and cross-track errors are bounded and oscillatory, unlike the in-track error. The in-track drift rate estimated from Fig. 1 is -11 m in 15 orbits of the chief.

Under the two-body assumption ($J_2 = 0$), the in-track drift per orbit due to linearization error for a PCO is [10]

$$y = -\frac{9\pi\rho^2}{4a_0} (2 + \cos 2\alpha_0) \quad (13)$$

The drift predicted by Eq. (13) for the data of this example is -11.2 m in 15 orbits. Hence, the in-track drift seen from Fig. 1 is predominantly due to the linearization of the two-body relative gravitational acceleration.

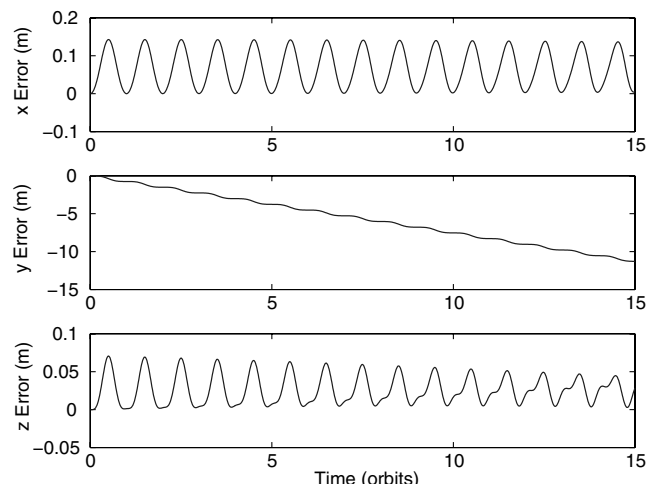


Fig. 1 Errors between the linear and nonlinear models (case 1, $\rho = 0.5$ km, $\alpha_0 = 0$ deg).

Case 2. The initial conditions for this example are for $\rho = 0.5$ km and $\alpha_0 = 90$ deg:

$$\begin{aligned} \delta\mathbf{r}(0) &= \\ &[0.250014418391 \ 0.000198338483 \ 0.500288022195]^T \text{ km} \\ \dot{\delta}\mathbf{r}(0) &= \\ &[-0.000000124335 \ -0.000527557529 \ -0.000000019840]^T \text{ km/s} \end{aligned}$$

The corresponding initial conditions of the deputy in the ECI frame are

$$\begin{aligned} \mathbf{r}_1 &= [5024.067715322 \ 5023.402914470 \ 0.171195964]^T \text{ km} \\ \mathbf{v}_1 &= \\ &[-1.810892863426 \ 1.810892391776 \ 7.040872374521]^T \text{ km/s} \end{aligned}$$

Figure 2 shows that, except for a change in the in-track drift rate, the error profiles are quite similar to those seen for the previous example. The radial error is predominantly oscillatory in nature, with a small superimposed linear growth rate. The in-track drift rate estimated from Fig. 2 is -3.5 m in 15 orbits, compared to -3.73 m during the same period, predicted by Eq. (13).

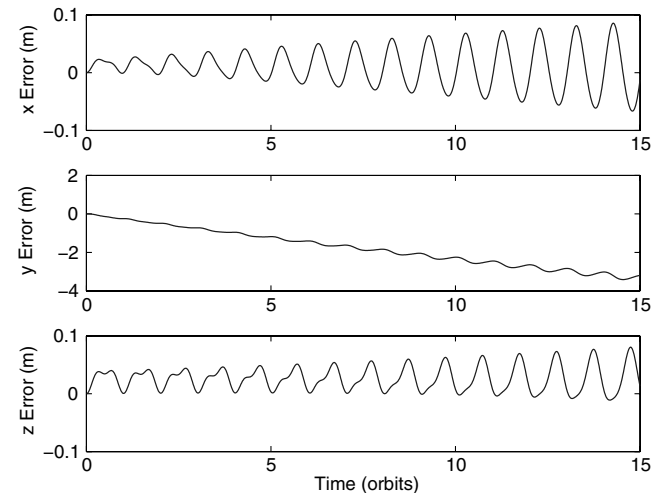


Fig. 2 Errors between the linear and nonlinear models (case 2, $\rho = 0.5$ km, $\alpha_0 = 90$ deg).

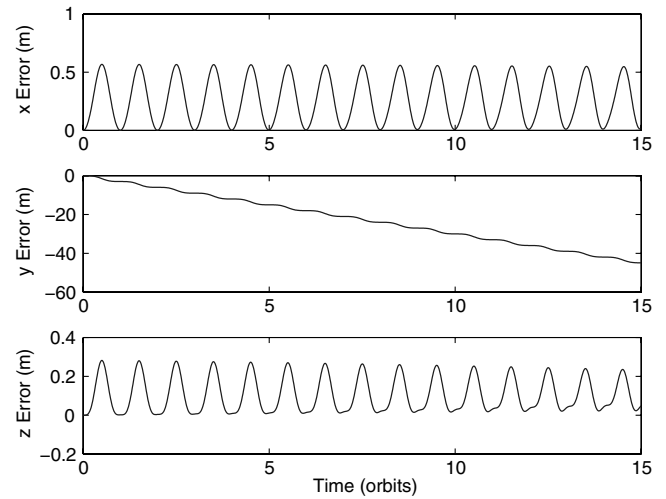


Fig. 3 Errors between the linear and nonlinear models (case 3, $\rho = 1$ km, $\alpha_0 = 0$ deg).

Cases 3 and 4. A PCO with $\rho = 1$ km is considered to show the effects of the size of the relative orbit on the model errors. Figures 3 and 4, respectively, show the errors between the linear and nonlinear simulations for $\alpha_0 = 0$ deg and $\alpha_0 = 90$ deg. The errors increase with the size of the orbit. The amplitudes of the radial and cross-track errors, as well as the in-track growth rate show quadratic relationships with ρ for $\alpha_0 = 0$ deg, as is to be expected from Eq. (13). The quadratic relationships of the error amplitudes with ρ are not well satisfied for $\alpha_0 = 90$ deg, showing a more dominant J_2 effect for this case.

Cases 5 and 6. The extent of the errors, solely due to the approximation of J_2 , can be ascertained by replacing the linear two-body differential gravitational acceleration of Eq. (6) by the difference of the two-body accelerations for the deputy and the chief, obtained from Eq. (5). The effect of this modification is evaluated for the 1 km PCO considered previously. Figure 5 shows the errors in the states with respect to the nonlinear simulation results for $\alpha_0 = 0$ deg and Fig. 6 shows the same for $\alpha_0 = 90$ deg. The in-track error due to the approximation of the J_2 effect is more for $\alpha_0 = 90$ deg as compared to that for $\alpha_0 = 0$, corroborating the conclusion drawn previously. However, the secular effect due to the J_2 approximation is very small compared with that due to linearization of the two-body differential gravitational acceleration.

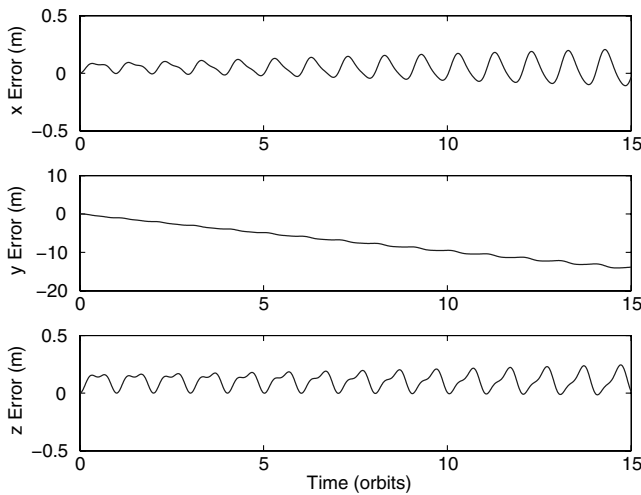


Fig. 4 Errors between the linear and nonlinear models (case 4, $\rho = 1$ km, $\alpha_0 = 90$ deg).

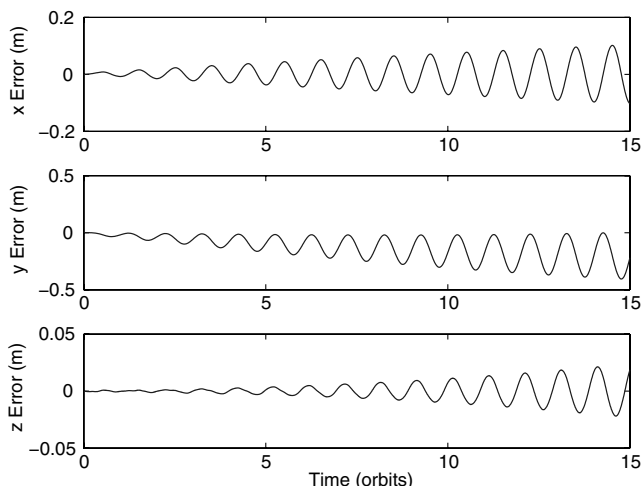


Fig. 5 Errors between the linear- J_2 -nonlinear two-body gravitational acceleration model and nonlinear simulation (case 5, $\rho = 1$ km, $\alpha_0 = 0$ deg).

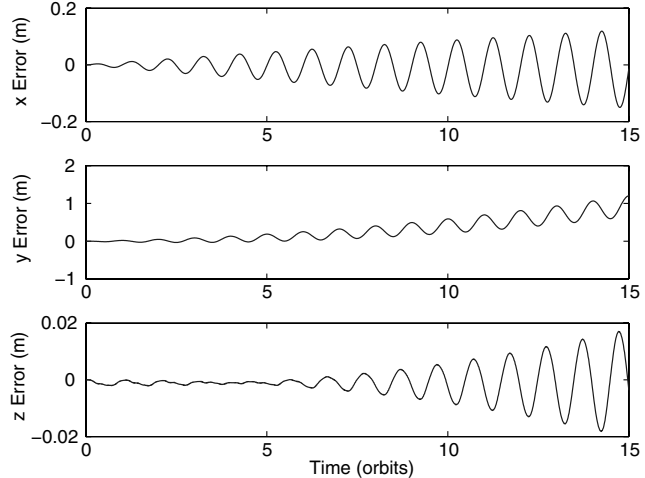


Fig. 6 Errors between the linear- J_2 -nonlinear two-body gravitational acceleration model and nonlinear simulation (case 6, $\rho = 1$ km, $\alpha_0 = 90$ deg).

Conclusions

A consistent linear model for J_2 -perturbed relative motion in the vicinity of a mean circular orbit has been developed. It accounts for the secular as well as short-period perturbation effects on the mean elements. The fidelity of the model has been verified on several test cases and by comparisons of the in-track errors with those associated with linearization of the two-body gravitational field. Results show that the primary source of error is due to linearization of the two-body gravitational field; the J_2 approximation is a secondary error source. The developed model can be used for rapid mission analysis and the design and evaluations of formation control strategies.

References

- [1] Vadali, S. R., Alfriend, K. T., and Vaddi, S. S., "Hill's Equations, Mean Orbital Elements, and Formation Flying of Satellites," *Advances in the Astronautical Sciences*, Vol. 106, March 2000, pp. 187–204, ISBN 0877034729; also American Astronautical Society Paper 00-258, 2000.
- [2] Ross, I. M., "Linearized Dynamic Equations for Spacecraft Subject to J_2 Perturbation," *Journal of Guidance, Control, and Dynamics*, Vol. 26, No. 4, July–Aug. 2003, pp. 657–659. doi:10.2514/2.5095
- [3] Schweigert, S. A., and Sedwick, R. J., "High-Fidelity Linearized J_2 Model for Satellite Formation Flight," *Journal of Guidance, Control, and Dynamics*, Vol. 25, No. 6, Nov.–Dec. 2002, pp. 1073–1080. doi:10.2514/2.4986
- [4] Izzo, D., Sabatini, M., and Valente, C., "A New Linear Model Describing Formation Flying Dynamics Under J_2 Effects," *Proceedings of the 17th AIDAA National Congress*, Vol. 1, Esografica, Rome, 2003, pp. 493–500.
- [5] Gim, D.-W., and Alfriend, K. T., "State Transition Matrix of Relative Motion for the Perturbed Noncircular Reference Orbit," *Journal of Guidance, Control, and Dynamics*, Vol. 26, No. 6, Nov.–Dec. 2003, pp. 956–971. doi:10.2514/2.6924
- [6] Hamel, J., and de Lafontaine, J., "Linearized Dynamics of Formation Flying Spacecraft on a J_2 -Perturbed Elliptical Orbit," *Journal of Guidance, Control, and Dynamics*, Vol. 30, No. 6, Nov.–Dec. 2007, pp. 1649–1658. doi:10.2514/1.29438
- [7] Born, G. H., Goldstein, D. B., and Thompson, B., "An Analytical Theory for Orbit Determination," *Journal of the Astronautical Sciences*, Vol. 49, No. 2, April–June 2001, pp. 345–361.
- [8] Sengupta, P., Vadali, S. R., and Alfriend, K. T., "Averaged Relative Motion and Applications to Formation Flight near Perturbed Orbits," *Journal of Guidance, Control, and Dynamics*, Vol. 31, No. 2, 2008, pp. 258–272. doi:10.2514/1.30620
- [9] Brouwer, D., "Solution of the Problem of Artificial Satellite Theory Without Drag," *Astronomical Journal*, Vol. 64, Nov. 1959, pp. 378–397.

doi:10.1086/107958

[10] Vaddi, S. S., Vadali, S. R., and Alfriend, K. T., "Formation Flying: Accommodating Nonlinearity and Eccentricity Perturbations," *Journal of Guidance, Control, and Dynamics*, Vol. 26, No. 2, 2003, pp. 214–223.
doi:10.2514/2.5054

[11] Vadali, S. R., Sengupta, P., Yan, H., and Alfriend, K. T., "Fundamental Frequencies of Satellite Relative Motion and Control of Formations," *Journal of Guidance, Control, and Dynamics*, Vol. 31, No. 5, 2008,
pp. 1239–1248.
doi:10.2514/1.34790

[12] Sengupta, P., and Vadali, S. R., "Relative Motion and the Geometry of Formations in Keplerian Elliptic Orbits," *Journal of Guidance, Control, and Dynamics*, Vol. 30, No. 4, 2007, pp. 953–964.
doi:10.2514/1.25941

[13] Vadali, S. R. H., Schaub, H., and Alfriend, K. T., "Initial Conditions and Fuel-Optimal Control for Formation Flying of Satellites," AIAA Paper 99-4265, Aug. 1999.